Published in final edited form as:
Nanomedicine (Lond). 2010 April ; 5(3): 361–368. doi:10.2217/nnm.10.6.

ChemoRad nanoparticles: a novel multifunctional nanoparticle platform for targeted delivery of concurrent chemoradiation

Andrew Z Wang[1,2], **Kai Yuet**[3], **Liangfang Zhang**[4], **Frank X Gu**[5], **Minh Huynh-Le**[3], **Aleksandar F Radovic-Moreno**[3], **Philip W Kantoff**[6], **Neil H Bander**[7], **Robert Langer**[3], and **Omid C Farokhzad**[1,3,†]

[1]Laboratory of Nanomedicine & Biomaterials, Department of Anesthesia, Brigham and Women's Hospital, Harvard Medical School, 75 Francis Street, Boston, MA, 02115, USA

[2]Harvard Medical School, USA

[3]Massachusetts Institute of Technology, USA

[4]University of California-San Diego CA, USA

[5]University of Waterloo, Waterloo, Canada

[6]Harvard Medical School, USA

[7]Weill Medical College of Cornell University New York, NY, USA

Abstract

Aim—The development of chemoradiation – the concurrent administration of chemotherapy and radiotherapy – has led to significant improvements in local tumor control and survival. However, it is limited by its high toxicity. In this study, we report the development of a novel NP (nanoparticle) therapeutic, ChemoRad NP, which can deliver biologically targeted chemoradiation.

Method—A biodegradable and biocompatible lipid–polymer hybrid NP that is capable of delivering both chemotherapy and radiotherapy was formulated.

Results—Using docetaxel, indium^{111} and yttrium^{90} as model drugs, we demonstrated that the ChemoRad NP can encapsulate chemotherapeutics (up to 9% of NP weight) and radiotherapeutics (100 mCi of radioisotope per gram of NP) efficiently and deliver both effectively. Using prostate cancer as a disease model, we demonstrated the targeted delivery of ChemoRad NPs and the higher therapeutic efficacy of ChemoRad NPs.

Conclusion—We believe that the ChemoRad NP represents a new class of therapeutics that holds great potential to improve cancer treatment.

Keywords

biologically targeted nanoparticle; ChemoRad NP; chemoradiation; chemoradiation nanoparticle; nanomedicine; nanotechnology; prostate cancer

[†]Author for correspondence Tel.: +1 617 732 6093 ofarokhzad@partners.org .

Financial & competing interests disclosure The authors have no other relevant affiliations or financial involvement with any organization or entity with a financial interest in or financial conflict with the subject matter or materials discussed in the manuscript apart from those disclosed.
No writing assistance was utilized in the production of this manuscript.

The advent of concurrent administration of chemotherapy and radiotherapy (chemoradiation) has significantly improved cancer care. Currently, it is the standard of treatment for many cancers, including esophageal, gastric, head and neck, and rectal cancers [1]. However, chemoradiation is limited by its higher (potentially life-threatening) toxicity, thereby precluding patients with poor general health from undergoing treatment. One potential strategy to improve chemoradiation utilizes advancements in drug delivery technology to improve efficacy and lower toxicity of the treatment. In particular, advances in nanotechnology have led to the development of nanoparticle (NP) drug-delivery vehicles, which can potentially improve the codelivery of chemoradiation. NPs are particularly well suited for cancer applications as they passively accumulate in tumors through the enhanced permeability and retention effect [2]. The proof-of-principle was observed in liposomal formulations of chemotherapeutics, such as Doxil, which demonstrated lower toxicity than their small molecular counterparts [3]. Our group and other investigators have demonstrated that the combination of biological targeting and NP delivery result in a higher concentration of chemotherapeutics within cancer cells [4–12]. Considering the many favorable characteristics of targeted NPs, we became interested in developing a targeted NP platform that is capable of delivering both chemotherapy and radiotherapy. We hypothesized that such an NP may improve efficacy and lower toxicity of chemoradiotherapy.

In this study, we report the development of what we believe to be the first multifunctional NP platform intended for the codelivery of chemotherapeutics and therapeutic radioisotopes (ChemoRad NP). Although previous studies have incorporated radioisotopes into NPs for biodistribution and pharmacokinetics, none have utilized the NPs for the delivery of chemoradiation [13]. The main challenge for engineering a ChemoRad NP lies in incorporating therapeutic doses of radioisotopes into NPs without affecting NP characteristics, including size, surface charge, stability and drug delivery profile. Potential compartments for radioisotope incorporation include the NP surface, the NP core, or a combination of the two. However, incorporating radioisotopes onto the NP surface would likely change the surface charge and size of the NP [14]. Furthermore, adding the radioisotopes into the core can change the drug encapsulation and drug release. Therefore, we chose to add radioisotopes into a layer between the outer NP surface and core. To accomplish this, we chose to utilize a lipid–polymer hybrid NP platform where such a layer is possible. The following design criteria were also used in the engineering of the ChemoRad NP [15]:

- The NP platform is comprised of natural or biocompatible and biodegradable/bioeliminable materials to facilitate potential clinical translation;
- The NPs should have minimal release of radioisotopes prior to reaching the tumor to minimize potential toxicity;
- The NPs should have size range of 50–100 nm, which has been shown to be optimal for tumor accumulation/targeting.

Based on these criteria, we developed the ChemoRad NP using a biodegradable poly ($_{D,L}$-lactic-co-glycolic acid) (PLGA) polymer and biocompatible lipids. We systematically examined the structural morphology, size, stability, drug release profile and radioisotope chelation properties of the ChemoRad NP, followed by evaluating its targeting ability and therapeutic effectiveness using prostate cancer as a disease model.

Materials & methods

Materials

All chemicals were obtained from Sigma-Aldrich (MO, USA) unless otherwise noted. The PLGA, 50/50 DL-lactide/glycolide, intravenous 0.55–0.75 (~50 kDa), was purchased from

Lactel (AL, USA). DSPE–PEG (1,2-distearoyl-sn-glycero-3-phosphoethanolamine-*N*-carboxy(polyethylene glycol) 2000, 1,2-dimyristoyl-sn-glycero-3-phosphoethanolamine-diethylene-triamine-pentaacetate (1,2-ditetradecanoyl-sn-glycero-3-phosphoethanolamine [DMPE]–diethylenetriaminepentaacetate [DTPA]) were purchased from Avanti Lipids (AL, USA). Lecithin (soybean, refined, molecular weight: ~330 Da) was purchased from Alfa Aesar (MA, USA). LNCaP and PC3 cell lines as well as tissue culture reagents were obtained from ATCC (Manassas, VA, USA). Indium-111 (half-life 2.83 days) and Yttrium-90 (half-life 2.67 days) were purchased from Perkin Elmers (MA, USA).

Synthesis & characterization of ChemoRad NP

Lipid–polymer hybrid ChemoRad NPs were prepared through a single-step nanoprecipitation method as previously described [16]. Briefly, the PLGA polymer was dissolved in acetonitrile at a concentration of 1 mg/ml. (Lecithin + DMPE–DTPA)/DSPE–PEG (8.5;1.5, molar ratio) with a weight ratio of 15% to the PLGA polymer was dissolved in 4% ethanol by weight aqueous solution. The DMPE-DTPA/lecithin molar ratio ranged from 1:85 (1% DMPE-DTPA surface) to 10:85 (10% DMPE–DTPA surface). The lecithin/DSPE-PEG/DMPE-DTPA solution was heated to 65°C to ensure all lipids were in liquid phase. The resulting PLGA solution was then added into the preheated lipid solution drop-wise under gentle stirring. The mixed solution was vortexed vigorously for 3 min followed by gentle stirring for 2 h at room temperature. The remaining organic solvent and free molecules were removed by washing the NP solution three times using an Amicon Ultra-4 centrifugal filter (Millipore, MA, USA) with a molecular weight cutoff of 10 kDa. To prepare drug-encapsulated NPs, docetaxel (Dtxl; Sigma-Aldrich, MO, USA) was dissolved into the PLGA acetonitrile solution before the nanoprecipitation process. We formulated NPs with 5–30% Dtxl by weight. To formulate aptamer (Apt) targeted NPs, the A10 Apt was first conjugated to DSPE–PEG through 1-ethyl-3-[3-dimethylaminopropyl] carbodiimide hydrochloride] (EDC) –*N*-hydroxysuccinimide (NHS) coupling reaction. The A10 Apt targets the prostate specific membrane antigen (PSMA) with high affinity and selectivity [17]. DSPE–PEG–COOH was first activated with EDC (25 μL, 400 mM) and sulfo-NHS (25 μL, 100 mM) for 15 min with gentle shaking in an aqueous solution. Amine terminated Apt (RNA-TEC, Belgium) was then added to the solution. The reaction was performed with gentle shaking for 4 h.

Characterization of ChemoRad NP

Nanoparticle size (diameter, nm) and surface charge (ζ-potential, mV) were obtained from three repeat measurements by quasi-elastic laser light scattering with a ζPALS dynamic light scattering detector (15 mW laser, incident beam = 676 nm; Brookhaven Instruments Corporation, NY, USA). NP size and shape distribution were further characterized using transmission electron microscopy. NP stability in serum was characterized by incubating 1 mg of NP in 10% human plasma solution and monitoring changes in NP size over time.

Drug loading & release study

In total, 3 ml of NP phosphate buffered saline (PBS) solutions at a concentration of 5 mg/ml were split equally into 30 Slide-A-lyzer MINI dialysis microtubes with a molecular weight cutoff of 3500 Da (Pierce, IL, USA). These microtubes were dialyzed in 4 l of PBS buffer at 37 °C with gentle stirring. PBS buffer was changed every 24 h during the whole dialysis process. At each data point, NP solutions from three microtubes were collected separately and mixed with an equal volume of acetonitrile to dissolve the NPs. The resulting free Dtxl content in each microtube was assayed using an Agilent (CA, USA) 1100 HPLC equipped with a pentafluorophenyl column (Curosil-PFP, 250 × 4.6 mm, 5 μm; Phenomenex, CA, USA). Dtxl absorbance was measured by a UV-Vis detector at 227 nm and a retention time of 12 min in 1 ml/min 50/50 acetonitrile/water mobile phase.

Chelation efficiency study

The ChemoRad NP and radioisotope chelation studies were carried out in 50 μM ammonium citrate buffer at pH 6. The chelation reactions were carried out in 37 °C for 45 min under gentle stirring. The chelation efficiency was measured by using a thin-layer chromatography protocol described by Cooper *et al*. [18]. Briefly, the Chemorad NPs chelated with radioisotopes were added to a thin-layer chromatographic strip and allowed to dry. The thin-layer chromatographic strip was then placed in a 5–10 ml of 0.1 M ammonium acetate, pH 6, containing 50 mM EDTA solution (mobile phase) in a 10- to 15-cm-tall glass beaker or similar container so that it is 0.5 cm deep. When the solvent is approximately 5 mm from the top of the strip, it was removed and dried. The strip was cut into two equal parts across the short axis. The radioactivity of the upper and lower halves were counted. The chelation efficiency was calculated by the percentage chelation efficiency equals counts on lower half of the strip divided by total counts, times 100 %.

Chelation stability study

ChemoRad NP solutions at a concentration of 5 mg/mL (100 μCi ^{111}In/mg and 5% Dtxl) were split equally into Slide-A-lyzer MINI dialysis microtubes with a molecular weight cutoff of 3500 Da. These microtubes were dialyzed in 4 l of PBS buffer at 37°C with gentle stirring. PBS buffer was changed every 24 h during the whole dialysis process. At each data point, NP solutions from three microtubes were collected separately. The ^{111}In content in the cells was assayed in a Packard Tri-Carb Scintillation Analyzer.

Fluorescence microscopy

To visualize cellular uptake of Apt targeted lipid–polymer hybrid NPs using fluorescence microscopy, a hydrophobic fluorescent dye, 22-(*N*-(7-nitrobenz-2-oxa-1,3-diazol-4-yl) amino)-23,24-bisnor-5-cholen-3-ol (NBD)-cholesterol (Invitrogen, CA, USA) was encapsulated. The fluorescence emission spectrum of NBD (excitation/emission = 460 nm/534 nm) was detected in the green channel (490 nm/528 nm) of a Delta Vision RT deconvolution microscope. Prostate cancer cell lines, LNCaP and PC3, were grown in eight-well microscope chamber slides to allow 70% confluence in 24 h (i.e., 40,000 cells per cm^2). NPs were added to achieve a final concentration of approximately 250 μg/ml (n = 4). Cells were incubated with the NPs for 45 min at 37°C, washed two times with PBS (300 μL per well), fixed with 4% formaldehyde, and mounted with nonfluorescent mounting medium 4′,6-diamidino-2-phenylindole (DAPI; Vector Laboratory, Inc., CA, USA). The 45 min time-point was chosen for the maximum observed difference between targeted NP uptake and nontargeted NP uptake experiments. The cells were then imaged using a deconvolution microscope (Delta Vision RT, Applied Precision, WA, USA).

MTS cell proliferation assay

LNCaP and PC3 cell lines were grown in 12-well plates to allow 70% confluence in 24 h (i.e., 40,000 cells/cm^2). Cells were incubated with the conjugates for 45 min at 37°C, washed and further incubated in fresh growth media for a total of 72 h. Cell viability was assessed colorimetrically with the 3-(4,5-dimethylthiazol-2-yl)-5-(3-carboxymethoxyphenyl)-2-(4-sulfophenyl)-2H-tetrazolium (MTS) reagent (Promega, CA, USA) following the standard protocol provided by the manufacturer. The absorbance was read with a microplate reader at 490 nm.

After identifying the Apt–ChemoRad–Dtxl (5% Dtxl by weight) LD_{50} concentration for the LNCaP cells, we used an MCNP 4C-Monte Carlo Code to calculate the amount of ^{90}Y for 6 Gy of radiation to each well [19]. Using È=0.646 MeV, $T = 2.59 \times 10^5$ s, $\lambda = 3.004 \times 10^{-6}$ s^{-1} and $m = 2.0 \times 10^{-3}$ kg (per well), the absorbed dose per initial activity was obtained as 9.3

$\times 10^{-6}$ Gy Bq^{-1}. This translated into 100 μCi ^{90}Y/mg NP for 50 μg of NP per well. For the *in vitro* efficacy study, the cells were incubated with ChemoRad NP (no Dtxl or ^{90}Y), Dtxl–ChemoRad NP, Apt–Dtxl–ChemoRad NP, Apt-Dtxl–^{90}Y–ChemoRad NP, Apt–^{90}Y–ChemoRad NP, and ^{90}Y–ChemoRad NP.

Results & discussion

To engineer the ChemoRad NP, we chose to modify the lipid–polymer NP platform, which has been shown to be an effective drug delivery vehicle [16]. Although there are several strategies to incorporate radioisotopes into NP, we chose to utilize a metal chelator given the high stability of metal radioisotope–chelator complex [20]. We added a lipid-chelator conjugate, DMPE–DTPA, into a lipid–polymer NP platform. The final ChemoRad NP is comprised of four main components:

- A hydrophobic polymeric core composed of PLGA that can be utilized to encapsulate poorly water soluble chemotherapeutics;
- A lipid monolayer composed of lecithin on the surface of the polymeric core to enhance drug retention;
- A hydrophilic polymeric shell composed of poly(ethylene glycol) (DSPE–poly [ethylene glycol]) to enhance stability and circulation half-life of the NP, as well as to provide a conjugation moiety to targeting ligands;
- A lipid chelator layer composed of DMPE-DTPA for the chelation of radioisotopes (Figure 1A).

To validate that the addition of the DMPE–DTPA did not change the characteristics of the lipid-polymer NP, the NP size and surface charge were examined with various concentrations of DMPE–DTPA. The mean hydrodynamic diameters and the ζ-potential of ChemoRad NPs with various DMPE–DTPA concentrations (1, 5 and 10%) were approximately 65 nm and approximately 35 mV respectively, and did not vary significantly with the DMPE-DTPA concentration (Table 1). Transmission electron microscopy confirmed the NPs are monodisperse spherical particles with sizes near 65 nm and a narrow size distribution (Figure 1b).

Nanoparticle stability *in vivo* is crucial to its effectiveness as a drug delivery vehicle. The ChemoRad NPs' stability (1, 5, and 10% DMPE–DTPA) was characterized in 10% plasma using the change in NP size as a surrogate for protein adsorption. PLGA NPs and lipid–polymer NPs without DMPE–DTPA were used as negative and positive controls, respectively. PLGA NPs are known to aggregate in plasma, whereas lipid–polymer NPs have been shown to be stable [21]. As seen in Figure 1C, while the PLGA NPs aggregated in plasma as expected, the ChemoRad NPs containing 1, 5 and 10% DMPE–DTPA maintained a stable size and did not aggregate. The external layer of PEG is known to prevent the adsorption of proteins and the interaction with the immune system [22].

To confirm that the addition of DMPE–DTPA did not vary the drug delivery capabilities of the lipid-polymer NP, we chose to use Dtxl as a model chemotherapeutic. The drug loading and drug encapsulation efficiency of the ChemoRad NP was quantified first. Using Dtxl to PLGA weight ratios from 5 to 30%, we found the ChemoRad NP encapsulation efficiency was approximately 60% (57–62%). The final drug load was up to 9% of the NP weight. Furthermore, the drug loading and encapsulation efficiency did not change with respect to DMPE–DTPA concentration (0, 1, 5 and 10%). Clinical Dtxl dose is 75 mg/m^2 weekly, which translates into a ChemoRad NP concentration of approximately 830 mg/m^2, a concentration achievable with the ChemoRad NP. Using ChemoRad NPs (5% DMPE–DTPA) containing 5% Dtxl by weight, we then studied the drug release profile of ChemoRad NPs. The 7-day

release profile showed controlled release of Dtxl with first-order release kinetics, as shown in Figure 2A. These results are consistent with the lipid-polymer NP platform as well as with other polymeric NP drug delivery platforms [8,23].

To demonstrate that ChemoRad NP is capable of delivering radiotherapy, we chose yttrium-90, a US FDA approved radiotherapeutic, as the model therapeutic radioisotope for our study [24]. ^{111}In, which is frequently utilized in place of ^{90}Y for experimentation and dose calculation, was used for the ChemoRad NP chelation studies [25]. The chelation efficiency of the ChemoRad NPs was identified using ChemoRad NPs (1, 5 and 10% DMPE–DTPA). Using 100 μCi of ^{111}In per 1 mg of NP, the chelation efficiency of the ChemoRad NPs was approximately 99% (98.7 ± 0.6%). We then conducted seven-day chelation stability studies, which showed that there is minimal release of the ^{111}In in the first 36 h and 80% of the dose was still retained after 60 h (Figure 2b). The subsequent release of ^{111}In is most consistent with NP degradation. Our results confirmed that the ChemoRad NP has high chelation efficiency and is capable of delivering clinical doses of radiotherapeutics (~100 mCi).

Our previous studies have demonstrated that the targeting ligand can promote intracellular uptake of the NPs, leading to higher intracellular drug accumulation within cancer cell [9,10]. As proof of principle, we used prostate cancer as a model disease and conjugated the A10 RNA Apt, which binds to the PSMA, to the ChemoRad NPs. We demonstrated target-specific uptake of Apt-targeted ChemoRad NPs using two prostate cancer cells lines, LNCaP (PSMA+) and PC3 (PSMA−) using *in vitro* visualization (Figure 3).

To quantify the preferential uptake of the targeted ChemoRad NPs as compared with non-targeted ChemoRad NPs, we chelated ^{111}In to the ChemoRad NPs and performed an *in vitro* cell uptake study. Radioactivity from LNCaP cells incubated with Apt–ChemoRad-^{111}In demonstrated that approximately 16% (15.8 ± 0.5) of the NPs was taken up by the cells within 45 min. Compared to the other experimental arms, the LNCaP cells incubated with Apt–ChemoRad-^{111}In had nearly ten times of the radioactivity as that of the others (Figure 4). Based on the differential uptake, targeted ChemoRad NP should improve efficacy and lower toxicity of chemoradiation.

We validated the therapeutic efficacy of ChemoRad NPs using ChemoRad NPs containing both Dtxl and ^{90}Y and the MTS cell survival assay. We chose to utilize NPs containing 5% DMPE–DTPA as each miligram of NP can chelate over 10 mCi of radioisotope. Using Apt-ChemoRad NPs encapsulating 5% Dtxl by weight, we first identified the LD_{50} Apt–ChemoRad–Dtxl concentration for the LNCaP cells, which was 25 mg/l (50 μg per well). We then calculated the amount of ^{90}Y chelate on ChemoRad NP that would result in approximately 6 Gy of radiation in each well. Based on the LD_{50} concentration of Apt–ChemoRad–Dtxl, the required concentration of ^{90}Y is 100 μCi per milligram of NP. Using ChemoRad NPs alone without the addition of Dtxl or ^{90}Y as negative controls, we incubated the LNCaP cells and PC3 cells with Dtxl–ChemoRad NP, Apt–Dtxl– ChemoRad NP, Apt–Dtxl–^{90}Y–ChemoRad NP, Apt–^{90}Y–ChemoRad NP and ^{90}Y-ChemoRad NP. As demonstrated in Figure 5, the targeted ChemoRad NP containing both chemotherapy and radiotherapy (Apt–Dtxl–^{90}Y–ChemoRad NP) has a dramatically higher level of cell killing of LNCaP cells when compared with targeted NPs containing single agent or nontargeted NPs.

Conclusion

In summary, we have developed what we believe to be the first NP platform that can deliver concurrent chemoradiation. The ChemoRad NP is composed entirely of biocompatible and biodegradable materials. We have shown that it has excellent physical characteristics as a drug delivery vehicle. We have also demonstrated that it can not only encapsulate and deliver

chemotherapy effectively, but also chelate therapeutic radioisotopes with high efficiency. Using the A10 Apt as a targeting ligand and prostate cancer as a model disease, we demonstrated that the ChemoRad NP can deliver concurrent chemotherapy and radiotherapy in a target-specific fashion, and the targeted concurrent chemoradiation from ChemoRad NP has much higher therapeutic efficacy than other forms of treatment. These data suggest that ChemoRad NP has the potential to be translated to clinical practice and improve chemoradiotherapy. Further research including *in vivo* experiments are required to validate the potential of ChemoRad NP.

Future perspective

We believe that the ChemoRad NP represents a novel class of therapeutics and has the potential to improve chemoradiation for cancer treatment. However, the *in vitro* results will need to be validated *in vivo*. We also believe this technology has the potential to make a significant impact on different fields of oncology, since the ChemoRad NP can be utilized for the treatment of many human cancers by functionalizing the NP with different targeting ligands.

Executive summary

- Our aim was to develop a novel nanoparticle (NP) platform that can deliver both chemotherapy and radiotherapy (chemoradiation).
- ChemoRad NP is a biodegradable, biocompatible NP capable of delivering both chemotherapeutics and radiotherapeutics efficiently.
- Using prostate cancer as a disease model, we demonstrated the biologically targeted ChemoRad NPs containing both chemotherapeutic and radiotherapeutic have higher therapeutic efficacy than nontargeted NPs and NPs containing a single therapeutic.
- We believe the ChemoRad NP represents a novel class of therapeutics and has the potential to improve chemoradiation for cancer treatment.

Acknowledgments

Omid C Farokhzad and Robert Langer have financial interest in BIND Biosciences and Selecta Biosciences. This work was supported by NIH Grants CA119349 (Robert Langer and Omid C Farokhzad) and EB003647 (Omid C Farokhzad); and the David Koch-Prostate Cancer Foundation Award in Nanotherapeutics (Robert Langer and Omid C Farokhzad).

Bibliography

Papers of special note have been highlighted as:

▪ of interest

▪▪ of considerable interest

1. Seiwert TY, Salama JK, Vokes EE. The concurrent chemoradiation paradigm – general principles. Nat. Clin. Pract 2007;4(2):86–100. ▪▪ Execellent review on chemoradiation, discussing the rationale of chemoradiotherapy, the clinical data on chemoradiation and why it is the standard of care for many different cancers.
2. Maeda H, Wu J, Sawa T, Matsumura Y, Hori K. Tumor vascular permeability and the EPR effect in macromolecular therapeutics: a review. J. Control. Release 2000;65(1–2):271–284. [PubMed: 10699287]

3. Sells RA, Owen RR, New RR, Gilmore IT. Reduction in toxicity of doxorubicin by liposomal entrapment. Lancet 1987;2(8559):624–625. [PubMed: 2887906] ▪ Clinical evidence of nanoparticle delivery lowering toxicity of the active small molecule agent.
4. Kim SH, Jeong JH, Chun KW, Park TG. Target-specific cellular uptake of PLGA nanoparticles coated with poly(l-lysine)-poly(ethylene glycol)-folate conjugate. Langmuir 2005;21(19):8852–8857. [PubMed: 16142970]
5. Oyewumi MO, Yokel RA, Jay M, Coakley T, Mumper RJ. Comparison of cell uptake, biodistribution and tumor retention of folate-coated and PEG-coated Gadolinium nanoparticles in tumor-bearing mice. J. Control. Release 2004;95(3):613–626. [PubMed: 15023471]
6. Bagalkot V, Farokhzad OC, Langer R, Jon S. An aptamer–doxorubicin physical conjugate as a novel targeted drug-delivery platform. Angew. Chem. Int. Ed. Engl 2006;45(48):8149–8152. [PubMed: 17099918]
7. Bagalkot V, Zhang L, Levy-Nissenbaum E, et al. Quantum dot-aptamer conjugates for synchronous cancer imaging, therapy, and sensing of drug delivery based on bi-fluorescence resonance energy transfer. Nano Lett 2007;7(10):3065–3070. [PubMed: 17854227]
8. Farokhzad OC, Cheng J, Teply BA, et al. Targeted nanoparticle-aptamer bioconjugates for cancer chemotherapy *in vivo*. Proc. Natl Acad. Nat. Sci. USA 2006;103(16):6315–6320. ▪▪ First publication demonstrating biologically targeted delivery of nanoparticles using aptamers on prostate cancer cells.
9. Farokhzad OC, Jon S, Khademhosseini A, Tran TN, Lavan DA, Langer R. Nanoparticle-aptamer bioconjugates: a new approach for targeting prostate cancer cells. Cancer Res 2004;64(21):7668–7672. [PubMed: 15520166]
10. Wang AZ, Bagalkot V, Vasilliou CC, et al. Superparamagnetic iron oxide nanoparticle–aptamer bioconjugates for combined prostate cancer imaging and therapy. ChemMedChem 2008;3(9):1311–1315. [PubMed: 18613203]
11. Zhang L, Radovic-Moreno AF, Alexis F, et al. Co-delivery of hydrophobic and hydrophilic drugs from nanoparticle–aptamer bioconjugates. ChemMedChem 2007;2(9):1268–1271. [PubMed: 17600796]
12. Kirpotin DB, Drummond DC, Shao Y, et al. Antibody targeting of long-circulating lipidic nanoparticles does not increase tumor localization but does increase internalization in animal models. Cancer Res 2006;66(13):6732–6740. [PubMed: 16818648]
13. Shenoy D, Little S, Langer R, Amiji M. Poly(ethylene oxide)-modified poly(β-amino ester) nanoparticles as a pH-sensitive system for tumor-targeted delivery of hydrophobic drugs: part 2. *In vivo* distribution and tumor localization studies. Pharm. Res 2005;22(12):2107–2114. [PubMed: 16254763]
14. Gabizon A, Chisin R, Amselem S, et al. Pharmacokinetic and imaging studies in patients receiving a formulation of liposome-associated adriamycin. Br. J. Cancer 1991;64(6):1125–1132. [PubMed: 1764376]
15. Perrault SD, Walkey C, Jennings T, Fischer HC, Chan WC. Mediating tumor targeting efficiency of nanoparticles through design. Nano Lett 2009;9(5):1909–1915. [PubMed: 19344179] ▪ Describes the optimal nanoparticle characteristics for therapeutic delivery to tumors.
16. Zhang L, Chan JM, Gu FX, et al. Self-assembled lipid-polymer hybrid nanoparticles: a robust drug delivery platform. ACS Nano 2008;2(8):1696–1702. [PubMed: 19206374] ▪▪ First description of the lipid–polymer hybrid nanoparticle platform.
17. Lupold SE, Hicke BJ, Lin Y, Coffey DS. Identification and characterization of nuclease-stabilized RNA molecules that bind human prostate cancer cells via the prostate-specific membrane antigen. Cancer Res 2002;62(14):4029–4033. [PubMed: 12124337]
18. Cooper MS, Sabbah E, Mather SJ. Conjugation of chelating agents to proteins and radiolabeling with trivalent metallic isotopes. Nat. Protoc 2006;1(1):314–317. [PubMed: 17406251]
19. Ljungberg M, Frey E, Sjogreen K, Liu X, Dewaraja Y, Strand SE. 3D absorbed dose : calculations based on spect: evaluation for ^{111}-In/^{90}-Y therapy using Monte Carlo simulations. Cancer Biother. Radiopharm 2003;18(1):99–107. [PubMed: 12667313]
20. Bhargava KK, Acharya SA. Labeling of monoclonal antibodies with radionuclides. Semin. Nucl. Med 1989;19(3):187–201. [PubMed: 2503873]

21. Zhang L, Chan JM, Gu FX, et al. Self-assembled lipid – polymer hybrid nanoparticles: a robust drug delivery platform. ACS Nano 2008;2(8):1696–1702. [PubMed: 19206374]

22. Ryan SM, Mantovani G, Wang X, Haddleton DM, Brayden DJ. Advances in pegylation of important biotech molecules: delivery aspects. Expert Opin. Drug Deliv 2008;5(4):371–383. [PubMed: 18426380]

23. Dong Y, Feng SS. Poly(d,l-lactide-co-glycolide) (PLGA) nanoparticles prepared by high pressure homogenization for paclitaxel chemotherapy. Int. J. Pharm 2007;342(1–2):208–214. [PubMed: 17560058]

24. Pohlman B, Sweetenham J, Macklis RM. Review of clinical radioimmunotherapy. Expert Rev. Anticancer Ther 2006;6(3):445–461. [PubMed: 16503861]

25. Press OW, Shan D, Howell-Clark J, et al. Comparative metabolism and retention of Iodine***$^{-125}$, Yttrium^{-90}, and Indium^{-111} radioimmunoconjugates by cancer cells. Cancer Res 1996;56(9):2123–2129. [PubMed: 8616860]

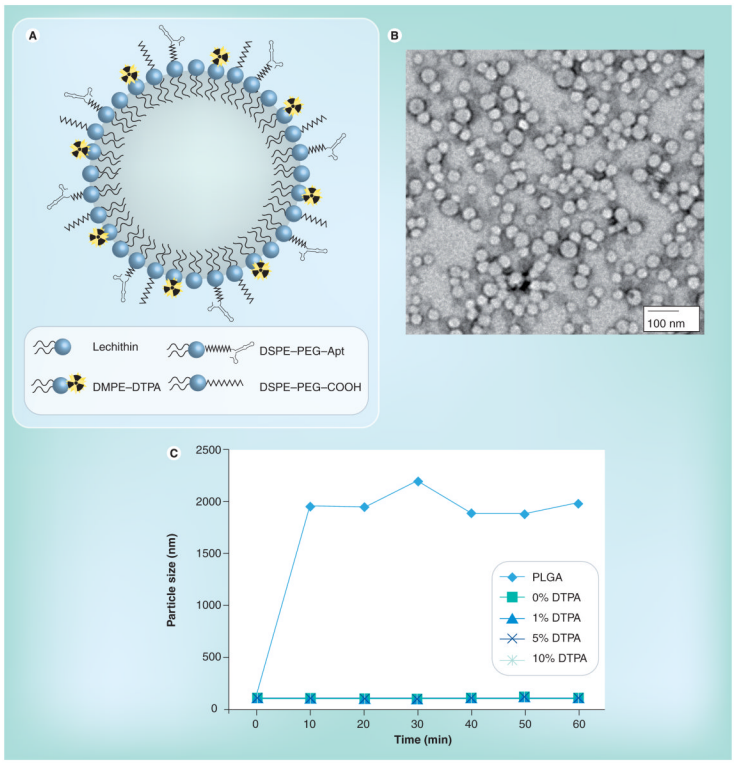

Figure 1.

(A) The ChemoRad nanoparticle (NP). **(B)** Transmission electron microscope of the ChemoRad NPs that contains 5% DMPE–DTPA. **(C)** *In vitro* stability study of ChemoRad NPs in 10% plasma. All ChemoRad NPs contain DSPE–PEG on their surface. Apt: Aptamer; DMPE: 1,2-ditetradecanoyl-sn-glycero-3-phosphoethanolamine; DSPE: Distearoylphosphatidylethanolamine-*N*-poly(ethylene glycol) 2000 (DSPE-PEG). DTPA: Diethylenetriaminepentaacetate; PEG: Poly(ethylene glycol); PLGA: Poly (d,l-lactic-co-glycolic acid).

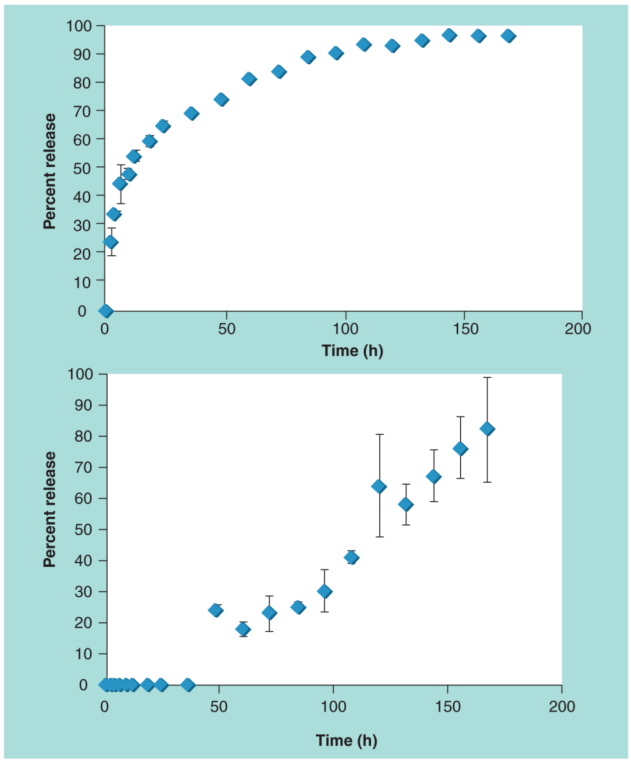

Figure 2. (A) 7-day docetaxel release study of docetaxel–ChemoRad nanoparticles
Drug loading was 5% docetaxel by weight **(B)** 7-day ^{111}In release study of ^{111}In-ChemoRad nanoparticles. 100 μCi of ^{111}In was chelated to each miligram of nanoparticle.

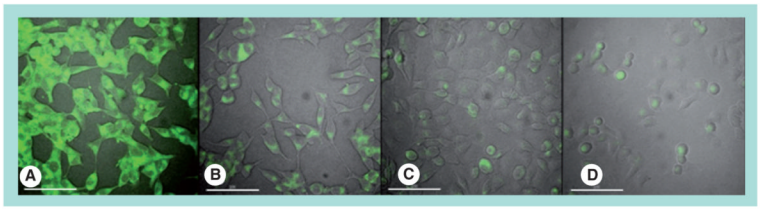

Figure 3. Selective binding and uptake of aptamer-targeted ChemoRad nanoparticles (NPs) in PC3 and LNCaP cells

Fluorescent dye 22-(N-(7-nitrobenz-2-oxa-1,3-diazol-4-yl)amino)-23,24-bisnor-5-cholen-3-ol (green) was encapsulated in NPs. A10 aptamer-targeted ChemoRad NPs were selectively delivered to PSMA–LNCaP cells **(A)**, but not to prostate specific membrane antigen–PC3 cells **(C)**. Nontargeted ChemoRad NPs had minimal uptake in either cell line **(B,D)**.

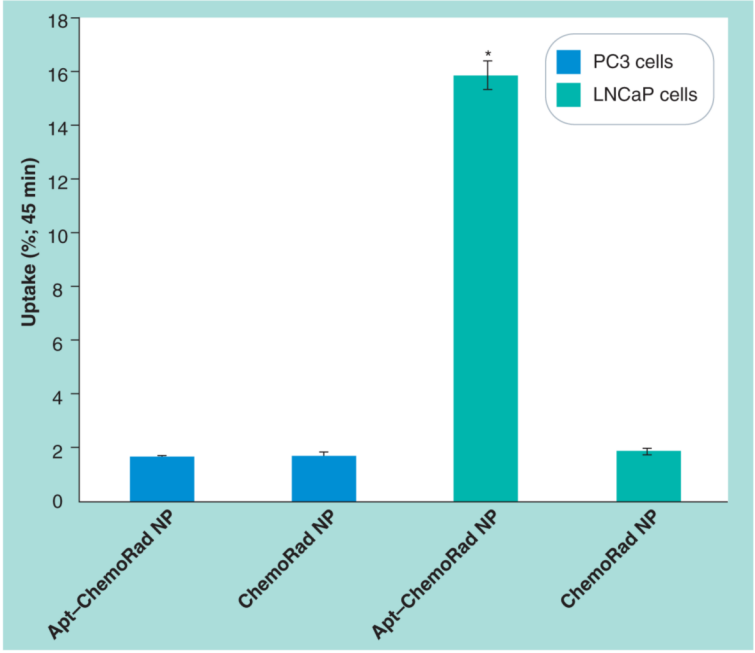

Figure 4. Selective binding and uptake of Apt-targeted ChemoRad nanoparticles with ^{111}In

A10 Apt-targeted ChemoRad NPs were selectively taken up by LNCaP cells but not by PC3 cells. Nontargeted ChemoRad NPs had minimal uptake in either cell line. *$p < 0.001$ using paired t-test.

Apt: Aptamer; NP: Nanoparticle.

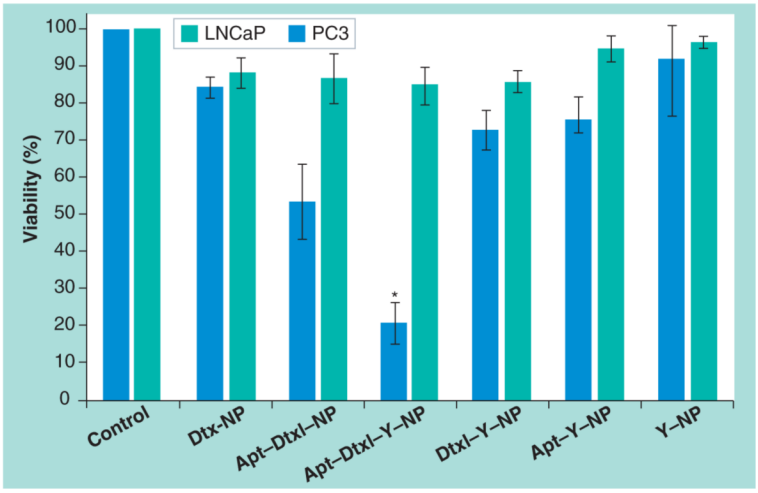

Figure 5. MTS cell viability assay of nanoparticles incubated with PC3 and LNCaP cells

Cells incubated with ChemoRad NPs without Dtxl or ^{90}Y were utilized as controls. Apt–Dtxl–^{90}Y–ChemoRad NPs (Apt–Dtxl–Y–NP) killed 80% of the LNCaP cells with minimal effects in PC3 cells.

*$p < 0.001$ using paired t-test.

Apt: Aptamer; Dtxl: Docetaxel; NP: Nanoparticle.

Table 1

Size and ζ potential of ChemoRad nanoparticles.

DTPA (%)	Mean particle size (nm)	ζ potential (mV)
0	66 ± 1	−34 ± 1
1	64 ± 2	−35 ± 1
5	66 ± 2	−34 ± 2
10	65 ± 1	−35 ± 1

DTPA: Diethylene-triamine-penta-acetate.